

Citrullination modulation stabilizes HIF-1 α to promote tumour progression

Chen *et al.*

Inventory of Supporting Information

1. Supplementary Figures and figures legends

Supplementary Fig. 1 | HIF-1 α is the substrate of PADI4-mediated citrullination. Related to Fig. 1.

Supplementary Fig. 2 | Identification of R698 residues as the conservative citrullination site on HIF-1 α among different species. Related to Fig. 2.

Supplementary Fig. 3 | PADI4 enzyme activity is required for HIF-1 α protein stabilization and transactivation. Related to Fig. 3.

Supplementary Fig. 4 | DHE inhibits tumour progression without bone marrow suppression and hepatic or renal toxicity in mice. Related to Fig. 5.

Supplementary Fig. 5 | HIF-1 α ^{R698} citrullination contributes to HCC tumorigenesis. Related to Fig. 6.

Supplementary Fig. 6 | HIF-1 α ^{R698} citrullination mediated by PADI4 promotes HIF-1 α protein stability and tumour progression.

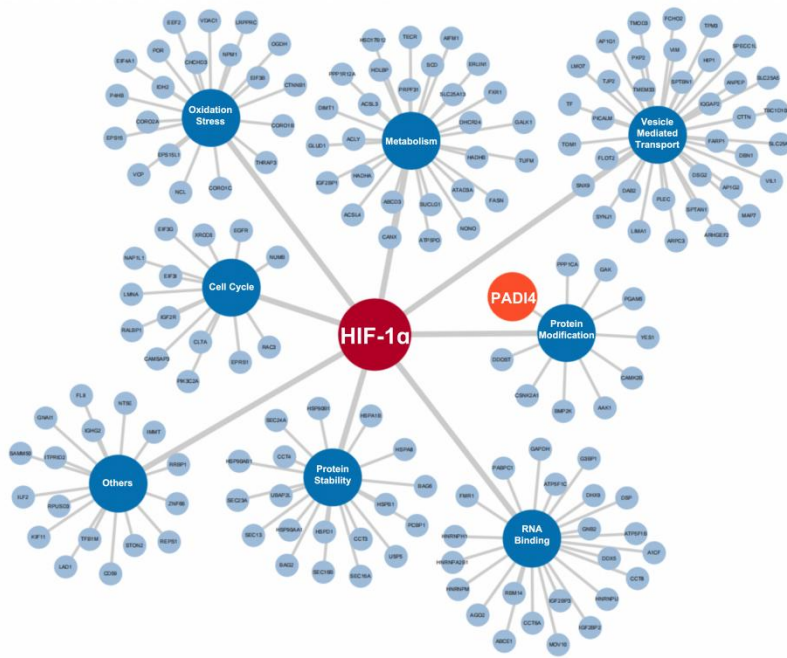
2. Supplementary Tables

Supplementary Tables 1. Oligonucleotide sequences of shRNA.

Supplementary Tables 2. Antibodies used in this study.

Supplementary Tables 3. Nucleotide sequences of primers used for quantitative real-time PCR.

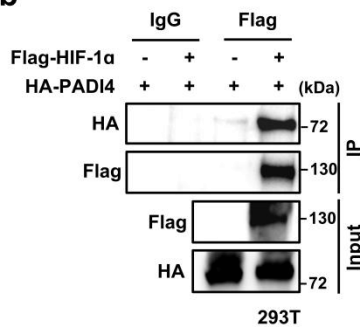
a



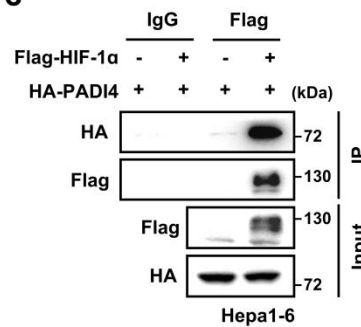
Unique peptides > 2 (Flag-HIF-1α vs Flag-EV)

Top10 proteins	Sum PEP Score	Unique Peptides
PIK3C2A	48.642	23
CORO1C	46.989	13
DAB2	41.489	13
PICALM	38.301	12
SPTAN1	37.922	14
SPECC1L	36.153	12
LIMA1	35.291	14
IGF2BP3	34.373	7
PADI4	32.588	7
HSPA8	32.481	10

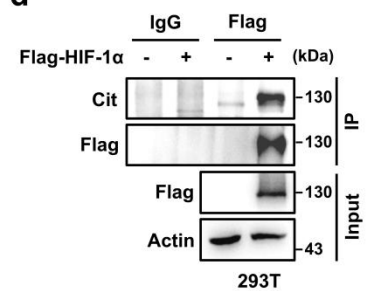
b



c

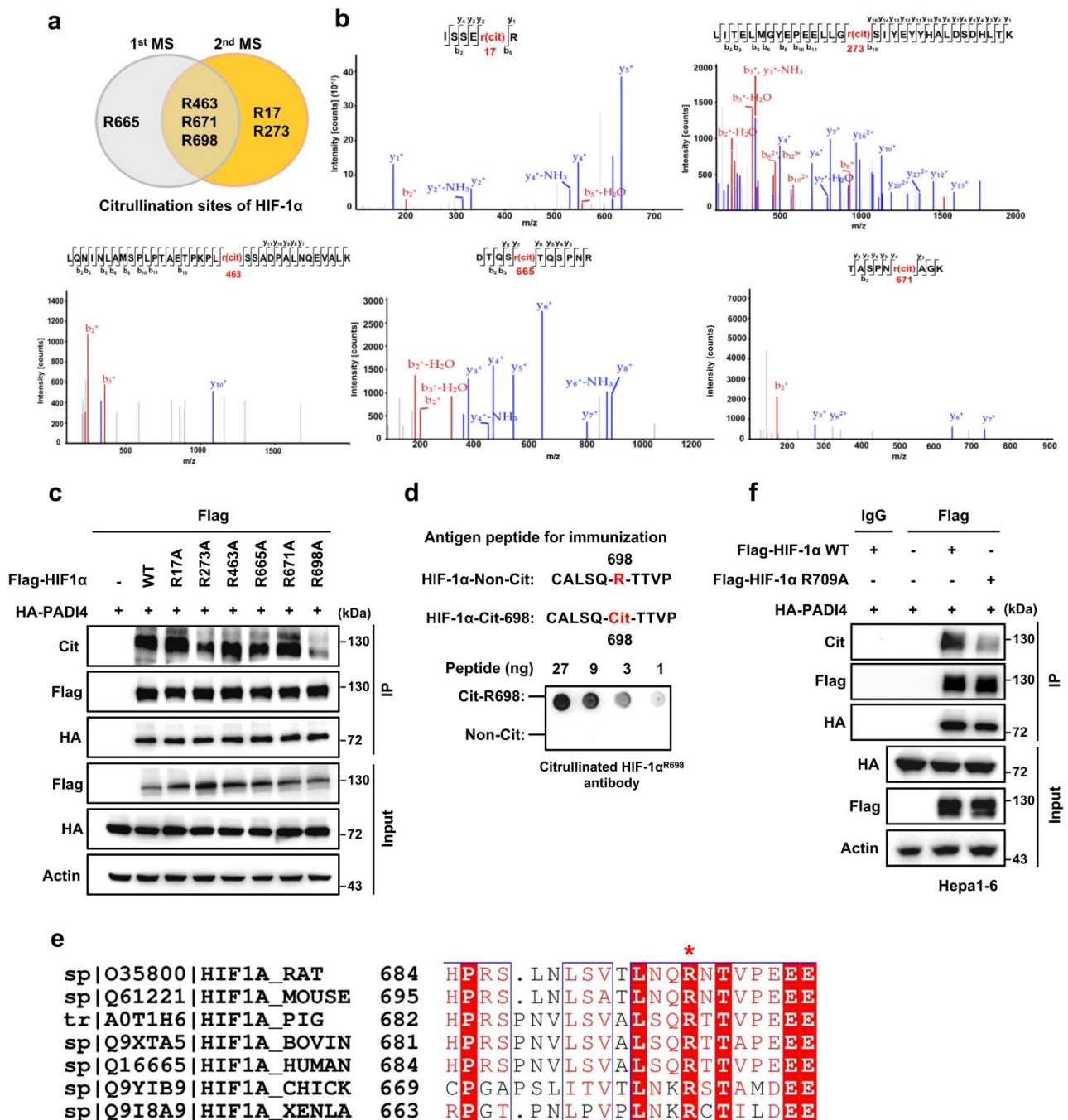


d



Supplementary Fig. 1 | HIF-1α is the substrate of PADI4-mediated citrullination. Related to Fig. 1.

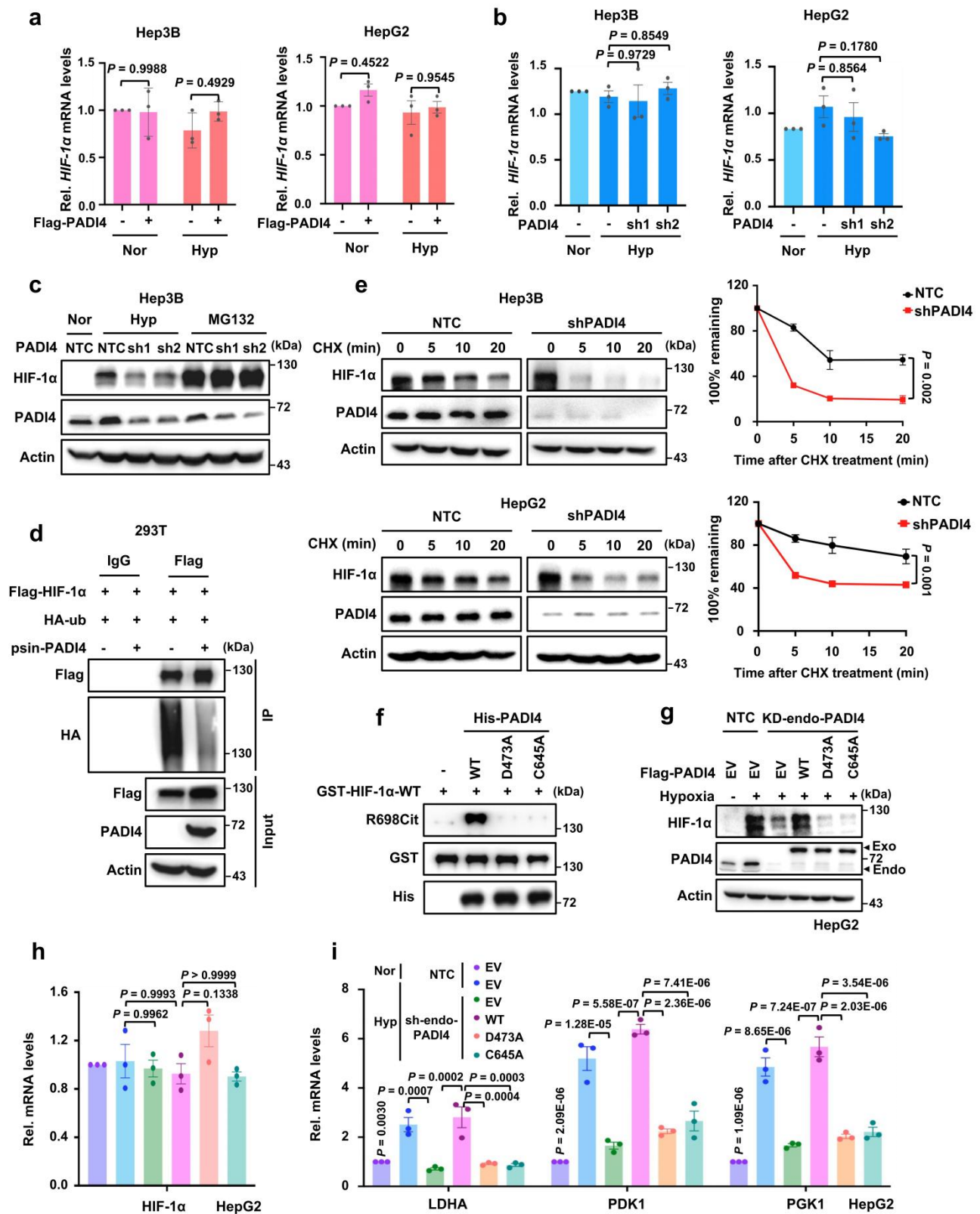
a, Analysis of proteins interacting with HIF-1α based on MS. Cytoscape 3.0 was used to visualize the complex network (left panel). The top 10 proteins according to Sum PEP (peptide) score and unique peptides interacting with HIF-1α are shown in the table (right panel). **b**, HEK293T cells were transfected with HA-PADI4 plasmid alone or with Flag-HIF-1α, followed by immunoprecipitation analysis. **c**, Hepa1-6 cells were transfected with HA-*mus-Padi4* plasmids alone or with Flag-*mus-Hif-1α* plasmids, followed by immunoprecipitation analysis. **d**, HEK293T cells were transfected with Flag-EV or Flag-HIF-1α plasmid, followed by western blotting analysis. The IP samples derive from the same experiment but different gels for Cit, another for Flag were processed in parallel. Immunoblots are representative of three independent experiments (**b-d**). Source data are provided as a Source Data file.



Supplementary Fig. 2 | Identification of R698 residues as the conservative citrullination site on HIF-1α among different species. Related to Fig. 2.

a, Venn diagram shows overlapping citrullination sites of HIF-1α as determined via two LC-MS/MS analysis. **b**, The citrullinated modification sites in HIF-1α including R17, R273, R463, R665 and R671 were determined by LC-MS/MS. **c**, HEK293T cells expressing Flag-HIF-1α WT, R17A, R273A, R463A, R665A, R671A or R698A together with HA-PADI4 were used for immunoprecipitation analysis. The IP samples derive from the same experiment but different gels for Cit, HA, another for Flag were processed in parallel. **d**, Validation of the citrullinated HIF-1α^{R698} antibody by dot blot using a nitrocellulose membrane spotted with citrullinated HIF-1α peptide with the R698 residue or the corresponding unmodified peptide at the indicated concentration. **e**, Primary sequence alignment of citrullinated peptides from the indicated species.

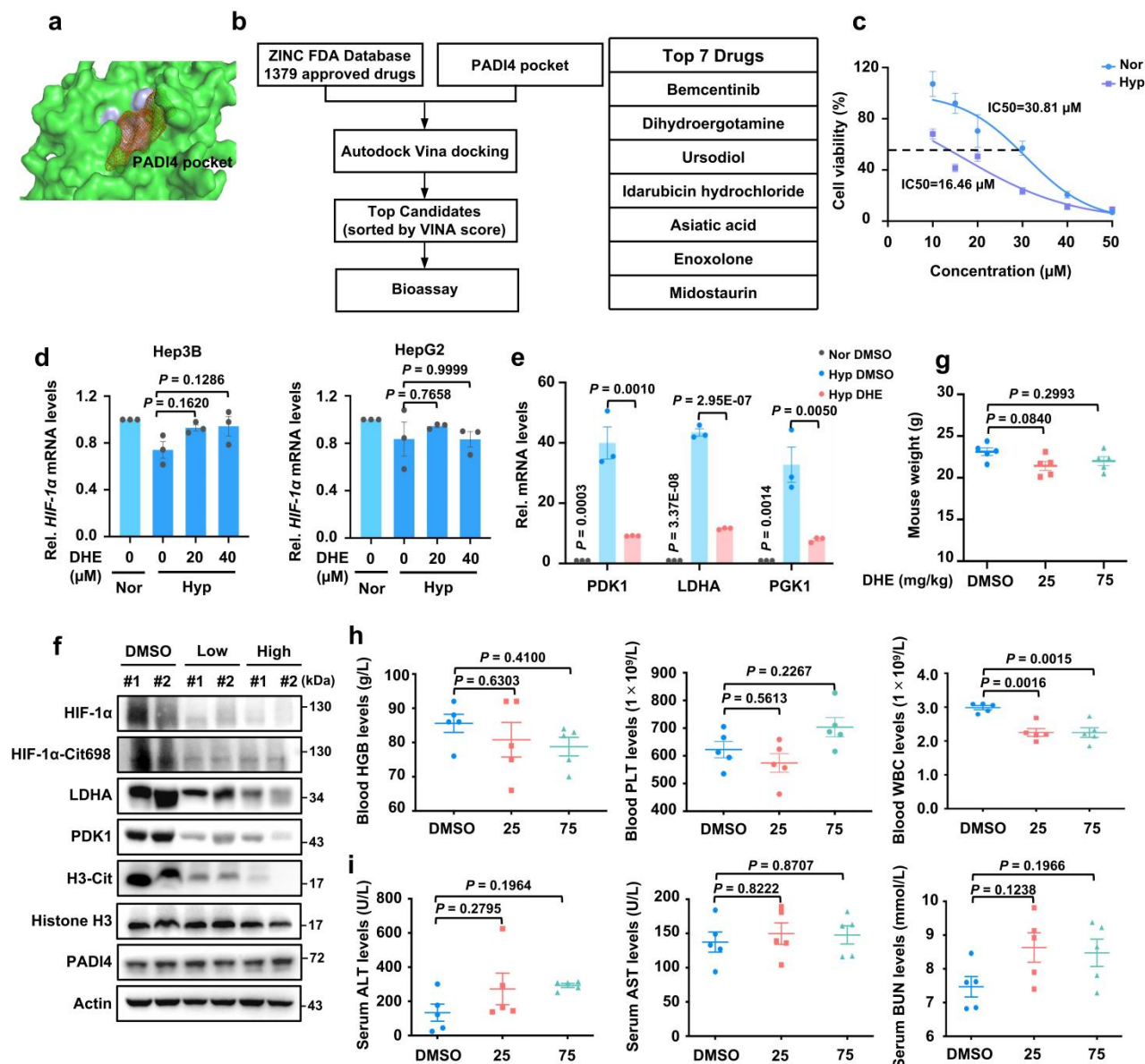
The * denotes the citrullinated R698 residue in *Homo sapiens* as detected by nano-LC-MS/MS. **f**, Hepa1-6 cells coexpressing Flag-*mus-Hif-1 α* ^{WT} or the Flag-*mus-Hif-1 α* ^{R709A} mutant together with HA-*mus-Padi4* were immunoprecipitated with an anti-Flag antibody followed by western blotting analysis. Immunoblots are representative of three independent experiments (**c,d,f**). Source data are provided as a Source Data file.



Supplementary Fig. 3 | PADI4 enzyme activity is required for HIF-1 α protein stabilization and transactivation. Related to Fig. 3.

a-b, qPCR measurement of *HIF-1 α* mRNA levels in Hep3B and HepG2 cells with PADI4 overexpressed (**a**) or knocked down (**b**) and cultured under normoxic or hypoxic conditions for 6 h. **c**, Western blot analysis of HIF-1 α and PADI4 protein levels in Hep3B cells expressing NTC or PADI4-shRNAs cultured under normoxic or hypoxic conditions in the presence or absence of 10

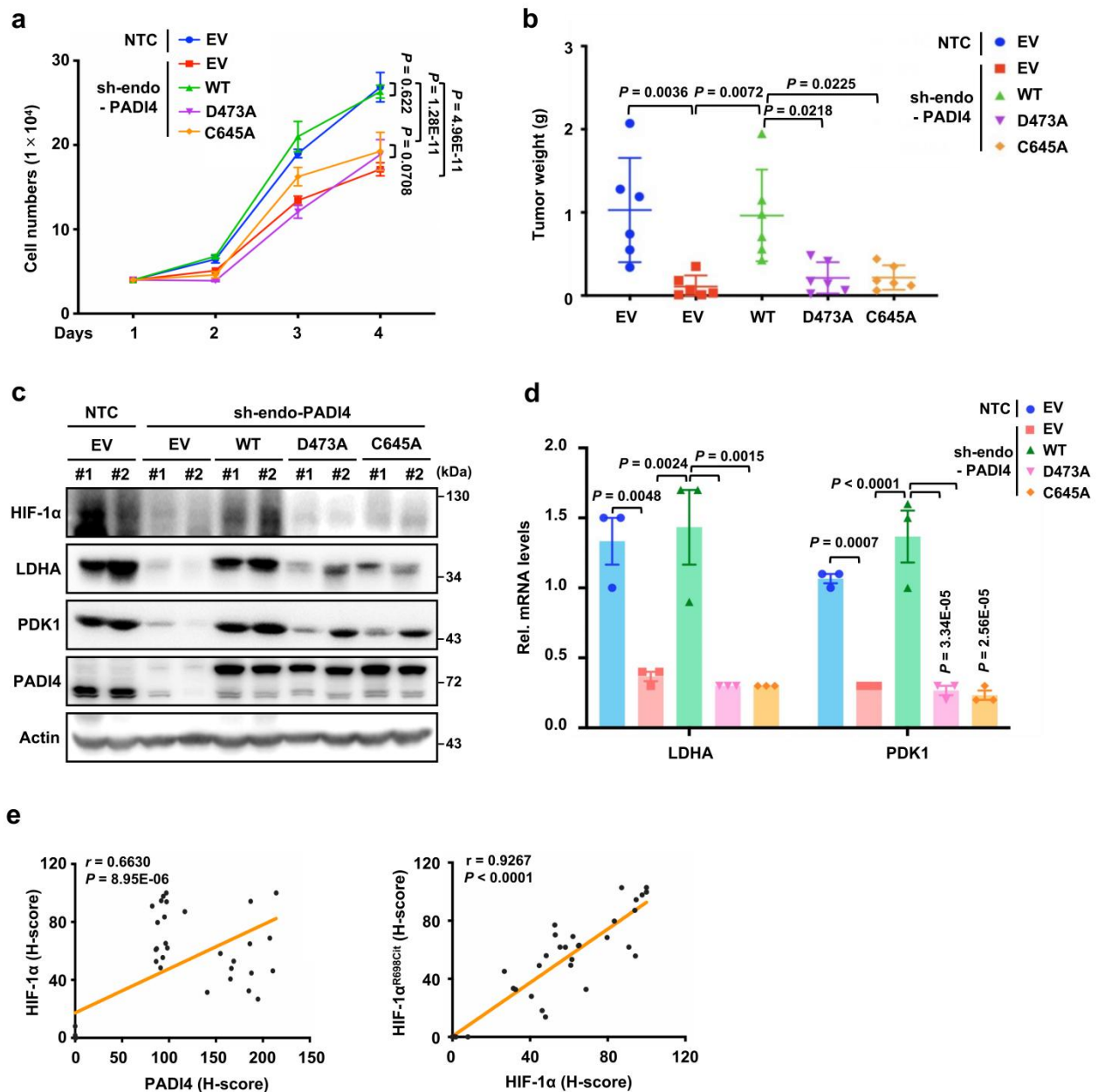
μ M MG132 for 6 h. **d**, HEK293T cells were transfected with EV or PADI4 plasmids and together with Flag-HIF-1 α and HA-Ub plasmids. After 48 h transfection, cells were treated by 10 μ M MG132 for another 6 h and followed by immunoprecipitation analysis. The IP samples derive from the same experiment but different gels for Flag, another for HA were processed in parallel. **e**, Western blotting analysis of HIF-1 α protein levels in Hep3B and HepG2 cells expressing NTC or PADI4 shRNA treated with 40 μ g/ml CHX for the indicated times (left panel). Quantification of HIF-1 α protein levels relative to Actin (right panel). **f**, An *in vitro* citrullination assay was performed by incubating purified GST-HIF-1 α with His-PADI4^{WT} or enzymatically inactivated His-PADI4^{D473A} or His-PADI4^{C645A} proteins at 37 °C for 1.5 h in the catalytic buffer and probing with the anti-HIF-1 α ^{R698Cit} antibody. The samples derive from the same experiment but different gels for R698Cit, His, another for GST were processed in parallel. **g-h**, Endogenous PADI4-knockdown HepG2 cells were infected with viruses expressing Flag-EV, Flag-PADI4^{WT}, Flag-PADI4^{D473A}, or Flag-PADI4^{C645A} and further cultured under normoxic or hypoxic conditions for 6 h. Cell lysates were harvested, and the protein and mRNA levels of HIF-1 α were analyzed by western blotting or qPCR, respectively. **i**, The cell lines described in **Figure S3g** were cultured under normoxic or hypoxic conditions for 24 h. The mRNA levels of *LDHA*, *PDK1*, and *PGK1* were analyzed by qPCR. Immunoblots are representative of three independent experiments (**c-g**). Data are presented as mean \pm S.E.M of three independent experiments (**a,b,e,h,i**). Statistical analyses were performed by ordinary one-way ANOVA (**a,b,h,i**) or two-way ANOVA test (**e**) with Turkey's multiple comparisons test. Source data are provided as a Source Data file.



Supplementary Fig. 4 | DHE inhibits tumour progression without bone marrow suppression and hepatic or renal toxicity in mice. Related to Fig. 5.

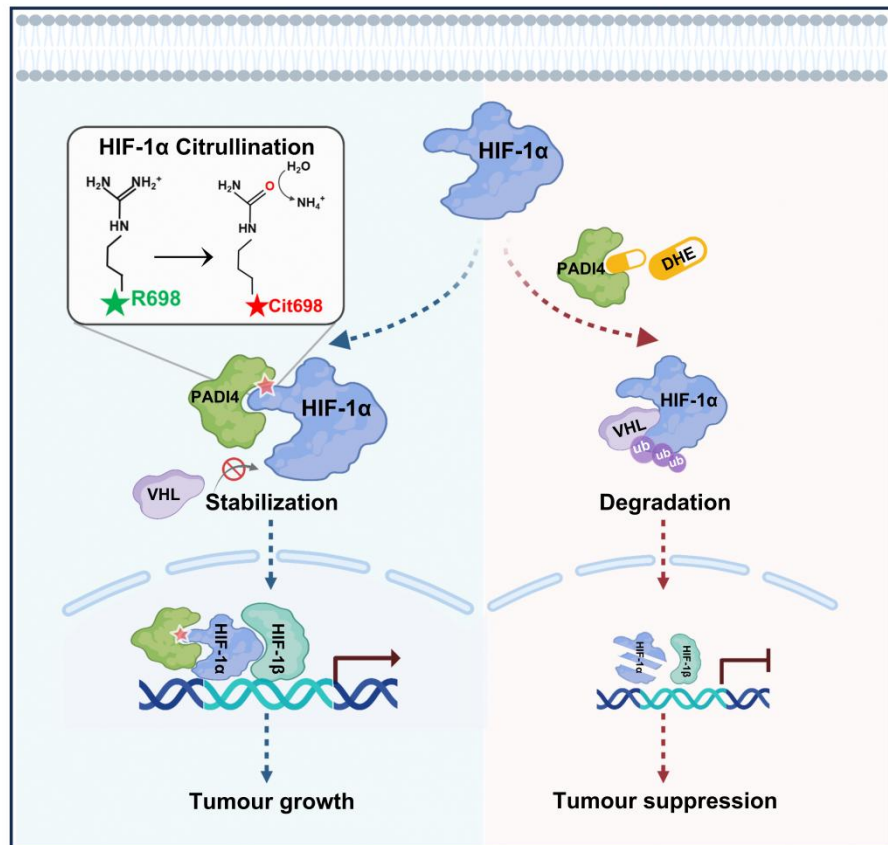
a, Crystal structure model of the enzymatic pocket of PADI4. **b**, Workflow of the PADI4 pocket-targeting drug screening (left). The top 7 drug candidates are shown (right). **c**, The viability of Hep3B cells treated with the indicated doses of DHE for 72 h under normoxic or hypoxic conditions was measured by cell counting assay. The IC₅₀ values of DHE were further calculated with GraphPad Prism 7.0. **d**, Hep3B and HepG2 cells treated with DMSO, 20 μM or 40 μM DHE were cultured under normoxic or hypoxic conditions for 6 h. The mRNA levels of *HIF-1α* were analyzed by qPCR. **e**, qPCR analysis of *PDK1*, *LDHA*, and *PGK1* mRNA levels in Hep3B cells treated with 20 μM DHE under normoxic or hypoxic conditions for 24 h. **f**, Western blotting analysis of PADI4, HIF-1α, HIF-1α^{R698Cit}, LDHA, PDK1, Histone3 (citrulline R2, R8, R17) and Histone3 protein levels in lysates of tumour tissues as described in **Figure 5m**. (**g-i**) Parental Hep3B cells were injected subcutaneously into the flanks of BALB/c nude mice ($n = 5$ mice per group). After 12 days, the mice were treated with DMSO or DHE (25 mg/kg or 75 mg/kg) by i.g every two days. The mice were sacrificed on Day 24. Weights of the mice were measured (**g**). Contents of

haemoglobin (HGB), platelets (PLTs), and white blood cells (WBCs) in the blood of the indicated xenograft model groups were measured with a Mindray blood cell analyzer (**h**). The concentration of alanine aminotransferase (ALT), aspartate aminotransferase (AST) and urea nitrogen (BUN) in the serum of the indicated xenograft model groups were measured with a HITACHI biochemical automatic analyzer (**i**). Error bars denote the mean \pm S.E.M. (**g-i**). Data are presented as mean \pm S.E.M of five (**c**) or three (**d,e**) independent experiments. Statistical analyses were performed by ordinary one-way ANOVA with Turkey's multiple comparisons test (**d-g,h,i**). Source data are provided as a Source Data file.



Supplementary Fig. 5 | HIF-1 α^{R698} citrullination contributes to HCC tumorigenesis. Related to Fig. 6.

a, Growth curves of the cells described in **Figure 3g** were determined by trypan blue counting. **b**, Tumour weights of xenograft mice described in **Figure 6b** were measured ($n = 6$ mice per group). Error bars denote the mean \pm S.E.M. **c**, Western blotting analysis of HIF-1 α , LDHA, PDK1, and PADI4 protein levels in the tumour tissue lysates described in **Figure 6b**. **d**, qPCR analysis of *LDHA* and *PDK1* mRNA levels in the tumour tissues lysates described in **Figure 6b**. **e**, HIF-1 α protein levels are positively correlated with PADI4 protein levels, and HIF-1 $\alpha^{R698Cit}$ protein levels are positively correlated with HIF-1 α protein levels in clinical HCC lesions ($n = 41$ patients' samples). Pearson correlation analyses were performed. Data are presented as mean \pm S.E.M of three independent experiments (**a,d**). Statistical analyses were performed by ordinary one-way ANOVA (**b,d**) or two-way ANOVA (**a**) with Turkey's multiple comparisons test or Pearson correlation analyses (**e**). Source data are provided as a Source Data file.

a

Supplementary Fig. 6 | HIF-1 α ^{R698} citrullination mediated by PADI4 promotes HIF-1 α protein stability and tumour progression.

a, Summary: PADI4-mediated HIF-1 α ^{R698} citrullination is a key modification in mediating HIF-1 α stability by preventing the VHL-HIF-1 α interaction, which is important for tumour growth. DHE, an inhibitor of PADI4, suppresses cancer cell proliferation and tumour growth by disrupting the interaction between HIF-1 α and PADI4 and thereby inducing HIF-1 α degradation. Supplementary Figure 6 created with BioRender.com is released under a Creative Commons Attribution-NonCommercial-NoDerivs 4.0 International license.

Supplementary Table 1. Oligonucleotide sequences of shRNA

Genes	Sequence
shVHL-1	CCGGTATCACACTGCCAGTGTATACCTCGAGGTATACACTGGCAGTGTGATATTT TTG
shPADI4-1	CCGGGCAAGAGCTCTTGTGAATATTCTCGAGAATATTCACAAGAGCTCTTGCTTT TTG
shPADI4-2	CCGGAGCAAGAGCTCTTGTGAATATCTCGAGATATTCACAAGAGCTCTTGCTTTT TTG

Supplementary Table 2. Antibodies used in this study

Antibodies	Source	Applications	Identifier
Mouse monoclonal anti-Citrulline (2D3.1)	Invitrogen	WB	MA5-27573
Mouse purified anti-HIF-1 α	BD Biosciences	WB	610959
Rabbit polyclonal anti-HIF-1 α (c-Term)	Cayman	IHC; IF	10006421
Mouse monoclonal anti-HIF-1 α	Novus Biologicals	IF	NB100-105SS
Rabbit polyclonal anti-HIF-1 α	Proteintech	IP	20960-1-Ap
Rabbit polyclonal anti-HIF-1 α ^{R698} citrullination	This study (Abclonal)	WB; IHC	WG-00942P
Rabbit polyclonal anti-PADI4	Abclonal	WB	A1906
Mouse monoclonal anti-PADI4	Abcam	IHC; IF	ab128086
Mouse monoclonal anti-His-tag	Proteintech	WB	66005-1-Ig
Mouse monoclonal anti-GST-tag	Proteintech	WB	66001-1-Ig
Rabbit polyclonal anti-HA-tag	Proteintech	IP	51064-2-Ap
Mouse monoclonal anti-HA-tag (6E2) (HRP Conjugate)	Cell Signaling Technology	WB	2999s
Mouse monoclonal anti-Flag-tag	Proteintech	WB; IP	66008-3-Ig
Mouse monoclonal anti-Beta Actin	Proteintech	WB	66009-1-Ig
Rabbit polyclonal anti-LDHA	Proteintech	WB	21799-1-AP
Rabbit polyclonal anti-PDK1	Proteintech	WB	18262-1-AP
Rabbit monoclonal anti-Hydroxy-HIF (Pro564) (D43B5)	Cell Signaling Technology	WB	3434s
Mouse monoclonal anti-VHL	Santa Cruz Biotechnology	WB	sc-135657
Rabbit polyclonal anti-Histone-H3	Proteintech	WB	17168-1-AP
Rabbit recombinant anti-Histone H3 (citrulline R2+R8+R17)	Abcam	WB	ab281584
Mouse IgG	Proteintech	IP	66360-1-Ig
Rabbit IgG	Proteintech	IP	30000-0-AP
Goat polyclonal anti-Mouse IgG (CoraLite594-conjugated)	Proteintech	IF	SA00013-3
Goat polyclonal anti-Mouse IgG (CoraLite488-conjugated)	Proteintech	IF	SA00013-1
Goat polyclonal anti-Rabbit IgG (CoraLite594-conjugated)	Proteintech	IF	SA00013-4
Goat polyclonal anti-Rabbit IgG (CoraLite488-conjugated)	Proteintech	IF	SA00013-2

Supplementary Table 3. Nucleotide sequences of primers used for quantitative real-time PCR

Name	Species	Forward primer	Reverse prime
HIF-1 α	<i>Homo sapiens</i>	ATCCATGTGACCATGAGGAAATG	TCGGCTAGTTAGGGTACTTTC
LDHA	<i>Homo sapiens</i>	GGCTACAACAGGATTCTA	TTACAAACCATTCTTATTTCTAAC
PDK1	<i>Homo sapiens</i>	ACCAGGACAGCCAATACAAG	CCTCGGTCACTCATCTTCAC
PGK1	<i>Homo sapiens</i>	GACCTAATGTCCAAAGCTGAGAA	CAGCAGGTATGCCAGAAGCC
18S rRNA	<i>Homo sapiens</i>	CGGCGACGACCCATTCGAAC	GAATCGAACCCTGATTCCCCGTC